Journal of Cellular Physiology

Molecular Mechanisms of p21 and p27 Induction by 3-Methylcholanthrene, an Aryl-Hydrocarbon Receptor Agonist, Involved in Antiproliferation of Human Umbilical Vascular Endothelial Cells

PAI-HUEI PANG,[1] YING-HSI LIN,[2] YI-HSUAN LEE,[2,3,4,5] HSING-HAN HOU,[6] SUNG-PO HSU,[7] AND SHU-HUI JUAN[2,3,4,5]*

[1]*Department of Ophthalmology, Shin-Kong Wu Ho-Su Memorial Hospital, Taipei, Taiwan*

[2]*Department of Physiology, Taipei Medical University, Taipei, Taiwan*

[3]*Graduate Institute of Medical Sciences, Taipei Medical University, Taipei, Taiwan*

[4]*Graduate Institute of Neuroscience, Taipei Medical University, Taipei, Taiwan*

[5]*Topnotch Stroke Research Center, Taipei Medical University, Taipei, Taiwan*

[6]*Institute of Biomedical Sciences, Academia Sinica, Taipei, Taiwan*

[7]*Institute of Physiology, College of Medicine, National Taiwan University, Taipei, Taiwan*

We previously reported that 3-methylcholanthrene (3MC), an aryl-hydrocarbon receptor (AhR) agonist, inhibits the proliferation of human umbilical vascular endothelial cells (HUVECs; Juan et al., 2006, Eur J Pharmacol 530: 1–8). Herein, pretreatment of HUVECs with p21 or p27 small interfering (si)RNA reduced 3MC-induced elimination of [^{3}H]thymidine incorporation, demonstrating their essential roles in the antiproliferation of HUVECs. The molecular mechanisms of p21 and p27 involved in the antiproliferative effects of 3MC were elucidated in this study. 3MC time- and concentration-dependently increased p21 and p27 levels, and decreased the protein level of CDK2 with no apparent alteration of p53. Interestingly, 3MC-mediated p21 and p27 inductions were eliminated by resveratrol, an AhR antagonist, suggesting their AhR dependency, further confirmed by AhR siRNA. Among the relevant pathways, p38MAPK activation sustained the levels of p21 and p27 induced by 3MC, which was eliminated by AhR antagonists and *N*-acetylcysteine (NAC), an antioxidant. 3MC concentration-dependently enhanced not only the consensus dioxin-responsive element (DRE)-driven luciferase activity, but also the binding activity of the AhR to the putative DRE derived from the p21 and p27 promoters. A deletion of the DRE (−285/−270) in p21 (−2,300/+8) only partially alleviated the 3MC-induced luciferase activity unless NAC was added, suggesting that there may be a DRE-independent mechanism associated with oxidative stress. However, a deletion of the DRE (−660/−645) in p27 (−1,358/−100) almost completely abrogated the activation. Our study demonstrated that both the functional DRE and the phosphorylation of p38MAPK are essential for the induction of p21 and p27, resulting in the antiproliferative action of 3MC in HUVECs.

J. Cell. Physiol. 215: 161–171, 2008.

Abbreviations: HUVECs, human umbilical vascular endothelial cells; 3MC, 3-methylcholanthrene; AhR, aryl-hydrocarbon receptor; DRE, dioxin-responsive element; TCDD, 2,3,7,8-tetrachlorodibenzo-*p*-dioxin; siRNA, small interfering RNA; RV, resveratrol; α-NF, α-naphthoflavone; NAC, *N*-acetylcysteine.

Contract grant sponsor: Shin Kong Wu Ho-Su Memorial Hospital, Taiwan;
Contract grant number: SKH-TMU-96-08.
Contract grant sponsor: Center of Excellence for Clinical Trials and Research in Neurology Specialty.
Contract grant sponsor: Topnotch Stroke Research Center Grant, Ministry of Education.

*Correspondence to: Shu-Hui Juan, PhD, Graduate Institute of Medical Sciences, Department of Physiology, Taipei Medical University, 250 Wu-Hsing Street, Taipei 110, Taiwan.
E-mail: juansh@tmu.edu.tw

Received 18 May 2007; Accepted 20 August 2007

DOI: 10.1002/jcp.21299

The aryl-hydrocarbon receptor (AhR) is a ubiquitous cytosolic protein that binds environmental hormones including polycyclic aromatic hydrocarbons (PAHs) such as benzopyrene and halogenated derivatives such as 2,3,7,8-tetrachlorodibenzo-*p*-dioxin (TCDD; Ma and Whitlock, 1997). The AhR is a ligand-activated transcription factor that belongs to the basic helix-loop-helix/Per-Arnt-Sim (bHLH/PAS) transcription factor superfamily. When ligand-bound AhR complexes are subsequently translocated into the nucleus following their association with the nuclear Arnt (AhR nuclear translocator) protein, the AhR complex is converted into its high-affinity DNA-binding form. The heterodimer binds to the dioxin-responsive element (DRE) on gene enhancers to activate the transcription of target genes, most notably members of the cytochrome P450 (CYP) family such as cytochrome P4501A1 (CYP1A1; Denison and Whitlock, 1995; Hankinson, 1995; Whitlock et al., 1996). Biochemical and genetic evidence has indicated that the biochemical mechanism of action of TCDD and PAHs is mediated by the AhR, which elicits a wide range of biological effects, including alteration of metabolic pathways, immunological changes, cardiac dysfunction, hepatotoxicity, carcinogenicity, endocrine dysfunction, and neoplasia (Brouwer et al., 1995; Hankinson, 1995; Safe, 1995). Environmental contamination by TCDD has adversely affected wildlife, and concerns have been raised about its consequences for human health. The actions and molecular mechanisms of TCDD in various biological systems have been intensively examined. In addition, increasing evidence has shown that multiple mechanisms are involved in AhR-dependent cell cycle arrest in different cell types; however, the molecular mechanisms of its cardiovascular toxicity remain to be elucidated.

The neurotoxic mechanism of TCDD has been extensively elucidated. For instance, TCDD-induced inhibition of neuronal cell proliferation is due to the AhR-dependent arrest at the G1 phase of the cell cycle through enhanced expression of p27 and hypophosphorylation of the Rb protein (Jin et al., 2004). In addition to neuronal cells, TCDD has been shown to enhance cell cycle arrest through increased protein levels of p21 and p27 in MCF-7 tumor cells (Lee and Safe, 2001) and cell cycle arrest at the G1 phase or apoptosis under conditions of excessive damage in human ectocervical cells (Rorke et al., 1998; Lee and Safe, 2001). This growth inhibition is associated with the concomitant induction of p53. However, AhR-mediated cell cycle arrest by TCDD is not the only pathway, because an A78D mutant of the constitutively active AhR, which lacks the ability for DRE-dependent transcription, partially inhibited the growth of Jurkat T cells (Ito et al., 2004). This suggests that growth inhibition is mediated by AhR-dependent and DRE-independent mechanisms. Additionally, dioxin has been shown to induce the immediate-early protooncogenes *c-fos* and *c-jun* genes, by AhR-dependent and -independent pathways (Hoffer et al., 1996).

In addition to the AhR-mediated response, it has also been documented that 3MC-induced free radical generation leads to p53 activation and apoptosis in HepG2 hepatoma cells (Kwon et al., 2002) through activation of a p38 mitogen-activated protein kinase (p38MAPK) signaling pathway. Mitogen-activated protein kinases (MAPKs) are the major pathway for regulating numerous cellular processes involved in cell proliferation, differentiation, stress response, and cell death. Three major classes of MAPKs have been described: extracellular signal-regulated kinase (ERK; Gomez and Cohen, 1991), c-Jun N-terminal kinase (JNK; Davis, 1999), and p38MAPK (Han et al., 1994; Nebreda and Porras, 2000). Generally, ERK modulates the responses of cell differentiation, whereas JNK and p38MAPK are activated by stress-associated stimuli, such as heat shock, inflammation, ultraviolet light, and irradiation (Kyriakis and Avruch, 2001). Our laboratory recently demonstrated that 3MC concentration-dependently increases CYP1A1 induction in human umbilical vascular endothelial cells (HUVECs; Juan et al., 2006). Additionally, it has been demonstrated that cytochrome P450 enzymes (i.e., CYP1A1) with the aid of epoxide hydrolase convert most of the carcinogenic PAHs to various reactive dihydrodiol-associated electrophiles (diolepoxides and *o*-quinones; Shimada et al., 1996), producing oxidative stress which contributes to JNK and p38MAPK activation (Ng et al., 1998).

Resveratrol (RV), an important component of red wine, has been shown to act as an aryl-hydrocarbon receptor (AhR) antagonist, and to have antioxidative and anti-inflammatory activities. Several studies within the last few years have shown that RV provides protection against coronary heart disease due to its significant antioxidant properties (Bors and Saran, 1987; Afanas'ev et al., 1989; Martinez and Moreno, 2000).

We observed that the antiproliferative effect of 3MC in HUVECs is correlated with the upregulation of p21 and p27 protein levels. In this study, we attempted to unravel the underlying molecular mechanisms associated with AhR-dependent and concomitant oxidative stress-mediated signal transduction pathways.

Materials and Methods

3-Methylcholanthrene (3MC) was purchased from Sigma Chemical (St. Louis, MO). Rabbit polyclonal anti-phosphospecific extracellular signal-regulated kinase 1/2 (ERK1/ERK2), anti-phosphospecific p38MAPK, and anti-phophospecific c-Jun N-terminal kinase (JNK) antibodies were purchased from New England Biolabs (Beverly, MA). Anti-ERK1/ERK2, anti-p38MAPK, and anti-JNK antibodies were purchased from Santa Cruz Biotechnology (Santa Cruz, CA). Anti-p21, anti-p27, anti-p53, anti-CDK2 and anti-CDK4 antibodies were purchased from Transduction Laboratories (Lexington, KY). Dulbecco's modified Eagle's medium (DMEM), fetal bovine serum (FBS), and tissue culture reagents were obtained from Invitrogen (Carlsbad, CA). Protein assay agents were purchased from Bio-Rad (Hercules, CA).

Cell culture and media

Human umbilical vein endothelial cells (HUVECs) were isolated from umbilical cord veins by collagenase treatment as described previously (Jaffe et al., 1973) and grown in medium 199 (M199) supplemented with 10% FBS, ECGS (0.03 mg/ml), kanamycin (50 U/ml), and 50 units/ml heparin (Sigma) in a humidified 37°C incubator. After the cells had grown to confluence, they were disaggregated in a trypsin solution, washed with PBS, and mixed with M199 containing 10% FBS; the mixture was centrifuged at 125*g* for 5 min, resuspended, and then subcultured according to standard protocols. Cells from passages 5 to 9 were used.

RNA isolation and analysis of gene expression by real-time polymerase chain reaction (PCR)

Total RNA was prepared from cultures by directly lysing cells in extraction buffer (Trizol/phenol/chloroform), and mRNAs were reversed-transcribed into cDNA using oligo-dT and reverse transcriptase (Invitrogen). After the first-strand cDNA synthesis, it was used as a template and amplified by pairs of primers derived from p21 and p27 genes for RT-PCR and quantitative real-time PCR analysis. Sequences of the primer pairs for amplification of each gene were 5′-GGCAGACCAGCATGACAGATTT-3′ and 5′-GGCGGATTAGGGCTTCCTCT-3′ (for the p21 gene); 5′-CCACGAAGAGTTAACCCGGG-3′ and 5′-GTCTGCTCCACAGAACCGGC-3′ (for the p27 gene); and

5′-CCACCATGGAGAAGGCTGGGGCTCA-3′ and 5′-ATCACGCCACAGTTTCCCGGAGGGG-3′ (for the GAPDH gene). PCR amplifications were conducted using QPCR Master Mixture and SYBER Green-based detection™ systems (ABI; Applied Biosystems, Taipei, Taiwan) according to the manufacturer's instructions, with 100 nM primers and 100 ng of a cDNA template in a 20-μl reaction volume. Thermocycling was initiated by 2 min of decontamination at 50°C and 10 min of hot start at 95°C, followed by 40 cycles (95°C for 15 sec, 55°C for 30 sec, and 60°C for 60 sec) with a single fluorescent reading taken at the end of each cycle. Each run was completed with a melting curve analysis to confirm the specificity of amplification and lack of primer dimers. Ct values were determined by the ABI System Software using a fluorescence threshold manually set to 0.0160. Individual gene expression Ct values at various time points were normalized by subtracting the respective Ct value of a housekeeping gene, GAPDH, to obtain a calibrated ΔCt value. Experimental samples are presented as multiples of induction with respect to each control group at various time points.

AhR small interfering RNA (siRNA) preparation and transient transfection

AhR siRNA (GGUAAAAGGGCAAAUAAUGTT) duplexes were chemically synthesized by Ambion (Austin, TX), and p21 and p27 siRNAs were purchased from Santa Cruz. HUVECs were seeded in a 6-well plate and transfected with either 100 pmol of AhR siRNA (#106526, Ambion), p21 siRNA (Santa Cruz, sc-29427), p27 siRNA (Santa Cruz, sc-29429), scrambled control siRNA (#4611, Ambion), or GAPDH siRNA (#4624, Ambion) in a 100-μl volume with siPORT™NeoFX™. The efficiency of AhR silencing was analyzed by Western blotting of AhR, p21, p27, and p38MAPK protein levels after transfection for 24 h, followed by serum starvation for 24 h in M199 medium containing 2% FBS and then 3MC treatment for 2 or 6 h.

Western blot analysis

The antibodies p21, p27, p53, CDK2, and GAPDH, and total and phosphorylated MAPK subfamilies were included in the assay. To prepare whole-cell lysates, cells were washed twice with ice-cold phosphate-buffered saline (PBS), resuspended in ice-cold extraction buffer (10 mM Tris (pH 7.0), 140 mM NaCl, 5 mM DTT, 0.5% Nonidet P-40, 1 mM Na_3VO_4, 1 mM phenylmethylsulfonyl fluoride (PMSF), 1 μg/ml leupeptin, and 1 μg/ml aprotinin), incubated on ice for 30 min, and vortexed every 10 min followed by centrifugation at 12,000 rpm for 30 min at 4°C. Whole-cell lysates (80 μg) were electrophoresed on a 10% SDS–polyacrylamide gel and then transblotted onto a Hybond-P membrane (GE Healthcare, Hong Kong, China). Membranes were blocked in PBS containing 0.1% Tween-20 and 5% skim milk at room temperature for 30 min. For detection of p21, p27, p53, CDK2, GAPDH, and the total and phosphorylated MAPK subfamilies, blots were incubated with the indicated antibodies (with dilutions used according to the manufacturer's instructions), in blocking buffer for 1 h at room temperature. After three washes with PBS containing 0.1% Tween-20, blots were incubated with peroxidase-conjugated goat anti-rabbit immunoglobulin G (IgG)/anti-mouse IgG (1:2,000) for 1 h at room temperature, followed by another washing. Expression of protein was detected by an enhanced chemiluminescence system.

Immunoprecipitation

CDK2 was immunoprecipitated from 200 μg protein using the anti-CDK2 antibody (2 μg) and protein A plus G agarose beads (20 μg). The precipitates were washed five times with lysis buffer and once with PBS. The pellet was then resuspended in sample buffer (50 mM Tris (pH 6.8), 100 mM bromophenol blue, and 10% glycerol) and incubated at 90°C for 10 min before electrophoresis to release the proteins from the beads.

[^{3}H]Thymidine incorporation

As previously described (Jain et al., 1996), HUVECs at a density of 1×10^4 cells/cm^3 were applied to 24-well plates in growth medium (M199 plus 10% FBS). After the cells had grown to 70–80% confluence, they were rendered quiescent by incubation for 24 h in DMEM containing 2% FBS. The concentration of 3MC as indicated or dimethyl sulfoxide (DMSO) in 10% FBS was added to the cells, and the mixture was allowed to incubate for 24 h. During the last 4 h of the incubation with or without 3MC, [^{3}H]thymidine was added at 1 μCi/ml (1 μCi = 37 kBq). The incorporated [^{3}H]thymidine was extracted in 0.2 N NaOH and measured in a liquid scintillation counter.

Constructs of the DRE enhancer and p21/p27 promoter variants

A luciferase reporter plasmid driven by the DRE known to be activated by the AhR-Arnt complex was prepared for the assay. In brief, the oligonucleotide with a triple repeat of the DRE obtained from the rat CYP1A1 enhancer region (GAGTTGCGTGAGAAGAGCC) was cloned into the *Kpn*I and *Nhe*I sites of the pGL2-promoter vector (Promega, Madison, WI), and designated pGL2-3DRE.

The pWWP-luc plasmid containing the promoter of human p21 between positions −2,300 and +8 (p21(−2,300/+8)) was a gift from Dr. Vogelstein (Johns Hopkins University, Baltimore, MD; el-Deiry et al., 1993). The p21 promoter region was removed with *Hind*III and subcloned into the unique *Hind*III site present within the pGL3-basic vector (Promega). To generate a deletion mutation on the putative DRE (−285/−270) of p21(−2,300/+8), 2 pairs of sense and antisense primers containing *Kpn*I and *Xho*I, and *Bgl*II and *Hind*III restriction sites, respectively, were as follows: sense 5′-AGTGGTACCTGATTGGCTTTCTGGCCATC-3′ and antisense 5′-ATTCTCGAGAGGAGGGCACTTCCCTCCTC-3′ (−2,300/−285), and sense 5′-CGAAGATCTGGGACCGGCT-GGCCTG-3′ and antisense 5′-AAGCTTAAGGAACTGACTT-CGGCAGC-3′ (−270/+8). Two fragments generated by the PCR amplification by the primers described above were sequentially cloned into the *Kpn*I/*Xho*I and *Bgl*II/*Hind*III sites of the pGL3-basic vector.

A DNA fragment containing 1.2 kb of the human p27 promoter between positions −1,358 and +132 (p27(−1,358/+132)) was obtained by PCR using human HepG2 genomic DNA as the template. The sense and antisense primers were 5′-CAATGTCCATGGCCTTAACTGTGCTTGGGA-3′ (p27 sense-1) and 5′-TGTCTCTGCAGTGCTTCTCCAAGTCCCGGG-3′ (p27 antisense-1), respectively. The resulting PCR product cloned in the yTA-vector was removed by the *Kpn*I/*Sal*I, followed by subcloning into the pGL3-basic promoter vector via the *Kpn*I/*Xho*I site. To obtain the p27 mutant without the DRE (−660/−645), two primers flanking the putative DRE region were 5′-CCGGGAGATTGCTGGAGGGGTACTGCTGCC-3′ (p27 mutant antisense-2) and 5′-CCCCTCCAGCAATCTCCCGGCGGCGCTCGG-3′ (p27 mutant sense-2). Two p27 promoter fragments without the DRE were generated by the PCR amplification using two pairs of primers (p27 sense-1 and p27 mutant antisense-2, and p27 mutant sense-2 and p27 antisense-1), which were cloned into the yTA vector for subsequent cloning into the pGL3-based vector by the *Kpn*I/*Xho*I and *Hind*III sites. The identities of the above-described enhancer/promoter sequences were confirmed using an ABI PRISM 377 DNA Analysis System (Perkin-Elmer, Wellesley, MA).

Luciferase activity assay

For the reporter activity assay, cells were seeded in 24-well plates at a density of 5×10^4 cells/well. In brief, cells in each well were transiently transfected with 0.55 μg of plasmid DNA containing 0.05 μg of the human Renilla luciferase construct, phRL-TK, as an internal control (Promega), and 0.5 μg of pGL2-3DRE or

pGL3/p21/p27 promoter firefly luciferase (FL) using jetPEI™ (Polyplus-Transfection, San Marcos, CA) for HUVECs. After transfection (4 h), the medium was replaced with medium supplemented with 10% FBS, and incubation continued for another 20 h. Transfected cells were pretreated with AhR antagonists or an antioxidant, *N*-acetylcysteine (NAC), followed by an additional 3MC challenge for 2 or 6 h as indicated, and cell lysates were collected. Luciferase activities were recorded in a TD-20/20 luminometer (Turner Designs, Madison, WI) using a dual luciferase assay kit (Promega) according to the manufacturer's instructions. The experimental reporter luciferase activity was calculated by subtracting the intrinsic activity as measured for samples corresponding to the pGL2-promoter or pGL3-basic vector and then normalizing it to the transfection efficiency as measured by the activity derived from phRL-TK.

Electrophoretic mobility shift assay

The electrophoretic mobility shift assay (EMSA) was performed as described previously (Wung et al., 1997). To prepare nuclear protein extracts, HUVECs in 10-cm^2 dishes after treatment with 3MC for 2 h in various concentrations as indicated were washed twice with ice-cold PBS and scraped off into 1 ml PBS. After centrifugation of the cell suspension at 500*g* for 3 min, the supernatant was removed, and the cell pellets were subjected to NE-PER™ nuclear extraction reagents (Pierce, Rockford, IL) with the addition of 0.5 mg/ml benzamidine, 2 μg/ml aprotinin, 2 μg/ml leupeptin, and 2 mM PMSF. The subsequent procedures for the nuclear protein extraction followed the manufacturer's instructions. The fraction containing the nuclear protein was used for the assay or was stored at −70°C until use. The sequences of the oligonucleotides used were CAGCACGCGAGGTTCC and AGTCACGCGACCAGCC for the putative p21 and p27 DREs, respectively. The oligonucleotide was end-labeled with [γ-^{32}P] dATP. Extracted nuclear proteins (10 μg) were incubated with 0.1 ng of ^{32}P-labeled DNA for 15 min at room temperature in 25 μl of binding buffer containing 1 μg of poly(dI−dC). For competition with unlabeled oligonucleotides, a 100-fold molar excess of unlabeled oligonucleotides relative to the radiolabeled probe was added to the binding assay. The mixtures were electrophoresed on 5% non-denaturing polyacrylamide gels. Gels were dried and imaged by means of autoradiography.

Statistical analysis

Values are expressed as the mean ± SD The significance of the difference from the control groups was analyzed by Student's *t*-test or one-way ANOVA and Bonferroni's method as a post-hoc test. A value of $P < 0.05$ was considered statistically significant.

Results

Time-dependent induction of p21 and p27 by 3MC

Our laboratory previously showed that 3MC at a concentration of as low as 5 nM caused the inhibition of [^{3}H]thymidine incorporation and growth arrest at the G0/G1 phase of the cell cycle (Juan et al., 2006). In this study, we continued examining the related genes involved in cell cycle regulation including the cyclin-dependent kinase inhibitors (CKIs), p21 and p27. The time-dependent induction of p21 and p27 by 3MC in HUVECs was analyzed at both the mRNA and protein levels; these were harvested from HUVECs treated with 10 nM 3MC for 3, 6, 9, 12, or 24 h. Real-time PCR analysis of p21 and p27 showed that 3MC at a concentration of 10 nM significantly induced p21 and p27 induction. The RNA induction of p21 and p27 was observed at 3–12 h of treatment, but not at 24 h of treatment (Fig. 1A). Consistent with the time frames of mRNA upregulation by real-time PCR analysis, Western blot analysis demonstrated that the induction of p21 by 3MC were apparent at 3, 6, and 12 h, but only marginal at 9 and 24 h. The induction of p27 by 3MC was observed at 3 h and sustained up to 12 h, whereas there was no apparent difference after 24 h of treatment, the longest time point examined (Fig. 1B).

3MC-mediated alterations in cell cycle activity through an AhR-dependent pathway

In addition to the induction of p21 and p27 by 3MC shown in Figure 1, other proteins related to the cell-cycle regulation such as p53, CDK2, and CDK4, and their dependency on the AhR or oxidative stress were investigated. Figure 2A demonstrates that the induction of p21 and p27 by 3MC was abolished by RV as an AhR antagonist and antioxidant; however, p53 was not apparently altered upon 3MC challenge. Furthermore, protein levels of CDK2, but not CDK4 (data not shown), were decreased by 3MC and rescued by the addition of RV. In spite of the decrease in the CDK2 protein level by 3MC, formation of the CDK2-p21 and CDK2-p27 complexes increased in a concentration-dependent fashion (Fig. 2A). Furthermore, AhR siRNA was utilized to examine the molecular mechanism of p21 and p27 induction by 6 h of 3MC treatment. Data presented in Figure 2B show that the efficiencies of GAPDH and AhR knockdown were greater than 50%, and AhR knockdown significantly decreased p21 and p27 induction by 3MC to levels similar to the control groups.

Important roles of p21 and p27 in the antiproliferative action of 3MC in HUVECs

As illustrated in Figures 1 and 2, levels of the p21 and p27 proteins and formation of the CDK2-p21 and CDK2-p27 complexes concentration-dependently increased in 3MC-treated HUVECs, suggesting that the upregulation of p21 and p27 might be responsible for the 3MC-mediated inhibition of DNA synthesis in these cells. To further demonstrate that in 3MC-treated HUVECs, increased p21 and p27 expressions were correlated with the antiproliferation of HUVECs, the experiment illustrated in Figure 3 was carried out. [^{3}H]Thymidine incorporation decreased in the sample treated with 10 nM 3MC alone. The sample labeled 3MC + p21 siRNA was treated with 100 pmol of p21 siRNA, which blocked the expression of p21, while sample 3MC + p27 siRNA was treated with 100 pmol of p27 siRNA, which blocked the expression of p27. Efficiencies of siRNAs against p21 and p27 were shown in Figure 3A by Western blotting analysis. Treatment of HUVECs with p21 or p27 siRNA alone caused no significant changes in [^{3}H]thymidine incorporation into HUVECs (data not shown). Consequently, pretreatment of HUVECs with p21 or p27 siRNA partially reversed the 3MC-induced decrease in [^{3}H]thymidine incorporation by approximately 75–83%. Furthermore, the 3MC-induced inhibition of [^{3}H]thymidine incorporation of HUVECs was completely reversed by the combined administration of both p21 and p27 siRNA (Fig. 3B). Nevertheless, scrambled siRNA did not alter the 3MC-mediated decrease in DNA synthesis (data not shown).

Involvement of p38MAPK activation in 3MC-mediated p21 and p27 induction

It has been shown that reactive oxygen species (ROS) generated by CYP1A1, the downstream target of AhR, or by metabolites of 3MC induce activation of the p38MAPK pathway, resulting in caspase-3-dependent apoptosis (Kwon et al., 2002). To examine the 3MC-induced signaling pathway involved in cell cycle arrest, the effects of 3MC on the total and phosphorylated forms of ERK1/ERK2, JNK, and p38MAPK were evaluated. HUVECs were quiescent for 24 h in M199 medium containing 2% FBS, which was then replaced with medium containing 10% FBS and treated with DMSO, or 1 or 10 nM 3MC for 2, 6, and 12 h. Crude cell lysates were harvested and analyzed for phosphorylated and total MAPKs by Western

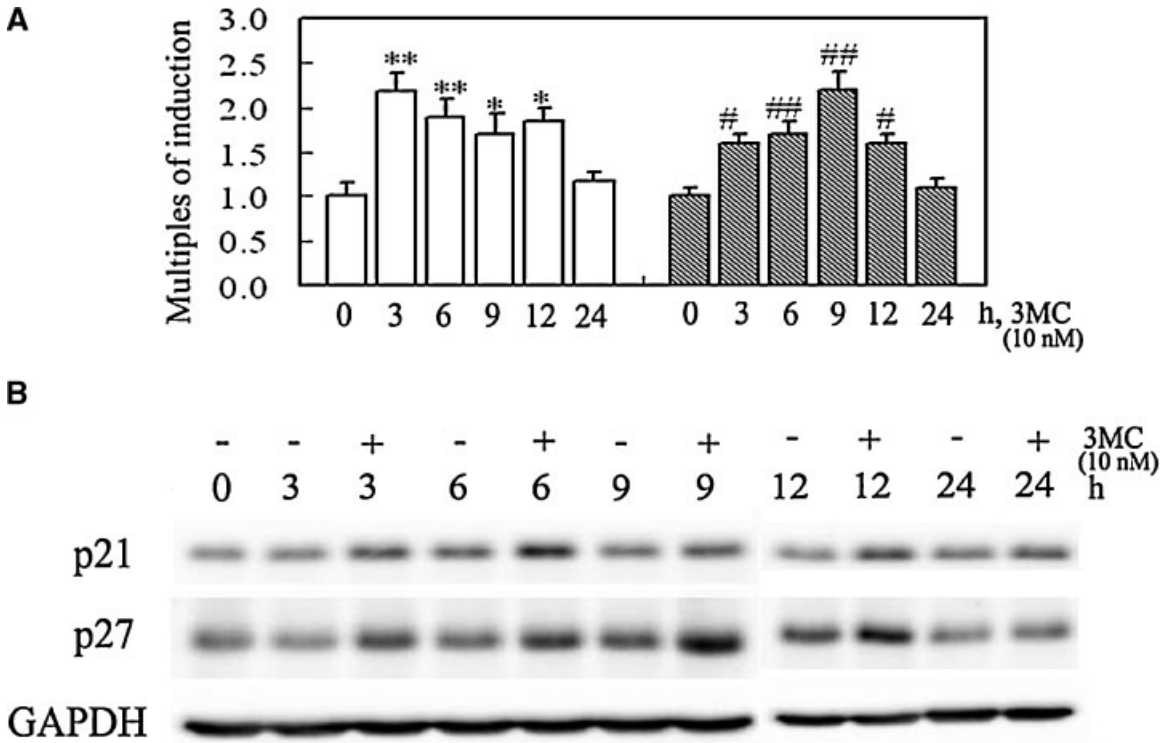

Fig. 1. Time-course induction of p21 and p27 by 3-methylcholanthrene (3MC) at the mRNA (A) and protein levels (B) in human umbilical vascular endothelial cells (HUVECs). Total RNA was extracted and analyzed by real-time PCR (A). Cells were treated with 3MC (10 nM) for 3, 6, 9, 12, and 24 h. Four samples were analyzed in each group, and values are presented as the mean ± SD. Significantly different ($^{*}P < 0.05$ and $^{**}P < 0.01$ vs. p21/GAPDH; $^{\#}P < 0.05$ and $^{\#\#}P < 0.01$ vs. p27/GAPDH). The protein levels of the 3MC-mediated p21 and p27 induction were assayed by Western blotting (B). Equal loading or transfer was confirmed by incubation with an anti-GAPDH antibody in (B). Representative results of three separate experiments are shown.

blotting. 3MC significantly stimulated the phosphorylation of p38MAPK at the indicated time points, but not at times <2 h (data not shown). One nanomolar of 3MC increased the extent of p38MAPK phosphorylation to about 1.5–2.0 times, while 10 nM of 3MC increased the phosphorylation to about 2.0–3.0 times at various time points of 2, 6, and 12 h, but not at times <2 h (data not shown). In contrast to p38MAPK, levels of total and phosphorylated ERK and JNK showed no significant changes in the control and treated cells with time (Fig. 4A). The underlying mechanisms of p38MAPK activation were examined using AhR antagonists and antioxidants including RV, α-naphthoflavone (α-NF), and NAC. Figure 4B demonstrates that activation of p38MAPK by 3MC was effectively blocked by RV, α-NF and NAC at 2 and 6 h following incubation as quantitated in the lower part of Figure 4B. Furthermore, the extent of p38MAPK inactivation by AhR knockdown was only approximately 15–25%, which was statistically significant lower than the extent of decrease in AhR expression by 50–60% (Fig. 4C), suggesting that an AhR-independent pathway also activates phosphorylation of p38MAPK.

Furthermore, MAPK inhibition experiments were performed to determine the role of p38MAPK in 3MC-mediated p21 and p27 gene induction. As shown in Figure 5A, 3MC-mediated p21 and p27 expressions were markedly attenuated by a p38MAPK inhibitor (SB202190) to the extent of a 40–60% reduction, but not by the respective inhibitors of ERK and JNK, U0126 and curcumin. We demonstrated that the activation of p38MAPK occurred at time points ≧2 h following 3MC treatment, and its inhibition by SB202190 eliminated the protein levels of p21 and p27, suggesting that p38MAPK might be involved in the induction of p21 and p27 by 3MC. Therefore, the time course of 3MC-mediated p21 and p27 induction in response to AhR antagonists and NAC was examined. In Figure 5B, RV effectively eliminated 3MC-induced p21 and p27 upregulation by about 40–50% at 2 and 6 h, whereas NAC only significantly decreased the upregulation by about 30–40% at the later time of 6 h. Conversely, α-NF decreased the induction of p21 and p27 at both time points, but statistical significance only occurred at the early time of 2 h.

Concentration-dependent binding activity of the AhR to the DRE by 3MC

The oligonucleotide with a triple repeat of the DRE synthesized from the rat CYP1A1 enhancer region was constructed into the pGL2 promoter vector, as described in "Materials and Methods Section." To investigate AhR-mediated gene transcription, HUVECs were transfected with a consensus DRE-driven luciferase construct, followed by an additional 1–100 nM of 3MC treatment. Interestingly, DRE-driven luciferase activity increased 3.0- to 5.0-fold by 3MC across the concentrations used, whereas it was significantly abolished by RV (Fig. 6A). Furthermore, the binding activities of the AhR to the DRE were further confirmed using an EMSA following 3MC treatment for 2 h, the probes of which were directly derived from the putative DRE enhancers of the human p21/p27 promoters. As demonstrated in Figure 6B, 3MC significantly increased the

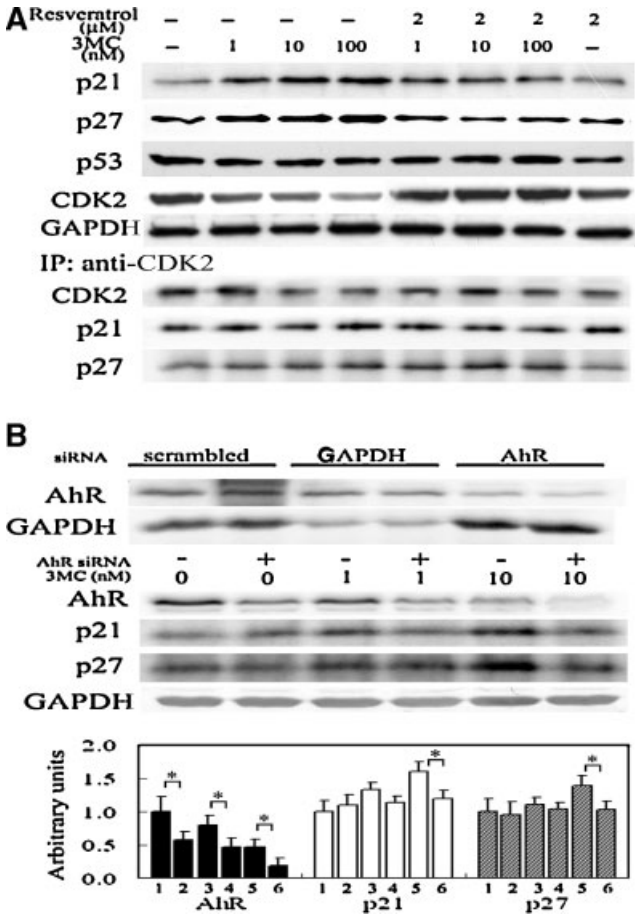

Fig. 2. Effects of resveratrol on 3MC-mediated cell cycle-related proteins and the action of 3MC in relation to the AhR in HUVECs. A: Cells were pretreated with 2 μM resveratrol for 1 h, prior to the addition of 3MC at the indicated concentrations for 6 h, and the protein levels of p21, p27, p53, and CDK2 were assayed by Western blotting. Membranes were probed with an anti-GAPDH antibody to verify equivalent loading. CDK2 was immunoprecipitated by the anti-CDK2 antibody, and the CDK2-p21 complex was detected with the anti-p21 antibody, whereas the CDK2-p27 complex was detected with the anti-p27 antibody. B: HUVECs were transfected with scrambled small interfering RNA (siRNA), GAPDH siRNA, or AhR siRNA for 24 h, followed by serum starvation for 24 h in M199 medium containing 2% FBS and 3MC treatment with the indicated concentrations for another 6 h. The expressions of AhR, GAPDH, p21, and p27 were analyzed by Western blotting. Representative results of three separate experiments are shown. Bar charts in the lower part of part B show the band intensities of the AhR, p21, and p27 normalized with GAPDH by densitometry. Data were derived from three independent experiments and are presented as the mean ± SD. $^{*}P < 0.05$ and $^{**}P < 0.01$ versus each respective control group.

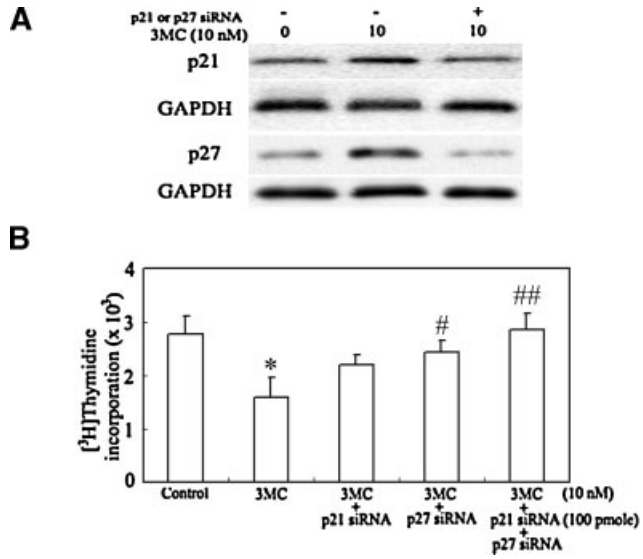

Fig. 3. Involvement of p21 and p27 in the 3MC-mediated decrease in [^{3}H]thymidine incorporation. A: Western blot analysis of p21 and p27 blocked by p21 and p27 siRNA. HUVECs were transfected with scrambled, p21, or p27 siRNA at a final concentration up to 100 pmol for 24 h, followed by serum starvation for 24 h in M199 medium containing 2% FBS and 10 nM 3MC treatment for an additional 24 h. B: Effects of p21 and p27 on cell proliferation in HUVECs. [^{3}H]Thymidine incorporation was carried out after the HUVECs were released from quiescence by incubation in culture media supplemented with 10% FBS and DMSO (control) or 10 nM 3MC in DMSO. Six samples were analyzed in each group, and values represent the mean ± SD. $^{*}P < 0.05$ versus the control. $^{\#}P < 0.05$ and $^{\#\#}P < 0.01$ versus the 3MC-treated group.

binding activities of the AhR to the putative DRE enhancers after 2 h of treatment of 3MC at the concentrations of 1 and 10 nM. We also provide evidence of specific DNA–protein complexes, because the 3MC-induced binding activities disappeared with competition from a 100-fold molar excess of unlabeled DRE oligonucleotides relative to the ^{32}P-labeled probes (Fig. 6B, lanes 5 and 11). Furthermore, AhR antibody (1.5 μg) was added to confirm the binding of AhR complex to p21- or p27-DRE probes in the presence of 3MC (10 nM), as shown in lanes 6 and 12 of Figure 6B. Instead of showing the antibody: AhR: DNA interaction (a supershift), gel-shift of the original AhR complex is disappeared in lane 6. Nevertheless it still confirms the identity of the AhR protein, since the binding of antibody to protein might interfere protein: DNA interaction using DRE probe derived from p21.

Inhibition of 3MC-mediated p21/p27 promoter-driven luciferase activity by deletion mutations

The promoter luciferase-reporter constructs spanning −2,300 to +8 and −1,358 to +132 of the human p21 and p27 promoter regions, respectively, were obtained and constructed into the pGL3-basic vector (Fig. 7A). These constructs were transiently transfected into HUVECs for 24 h followed by treatment with 2 μM RV or 1 mM NAC for 1 h prior to the addition of 3MC (10 nM) for 2 or 6 h. p21 (−2,300/+8) luciferase activity was increased 3.5- to 4.0-fold by 10 nM 3MC, whereas that of p27 (−1,358/+132) was enhanced 2.0- to 2.5-fold at the time points of 2 and 6 h. RV, an AhR antagonist, significantly blocked the 3MC-enhanced promoter activity of p21 (−2,300/+8) and p27 (−1,358/+132) at both time points. However, blockage of p21 promoter activity by NAC was only effective at 6 h, but not at 2 h, following treatment. In contrast, NAC was unable to decrease p27 (−1,358/+132) promoter activities following 3MC treatment at both 2 and 6 h (Fig. 7B).

Another approach consisting of deletion mutations was used to confirm the importance of the AhR binding site involved in 3MC-mediated p21/p27 promoter-driven luciferase activity (Fig. 7A). Following 3MC treatment for 6 h, the activity of the DRE-deleted p21 promoter (Dp21) was only partially alleviated

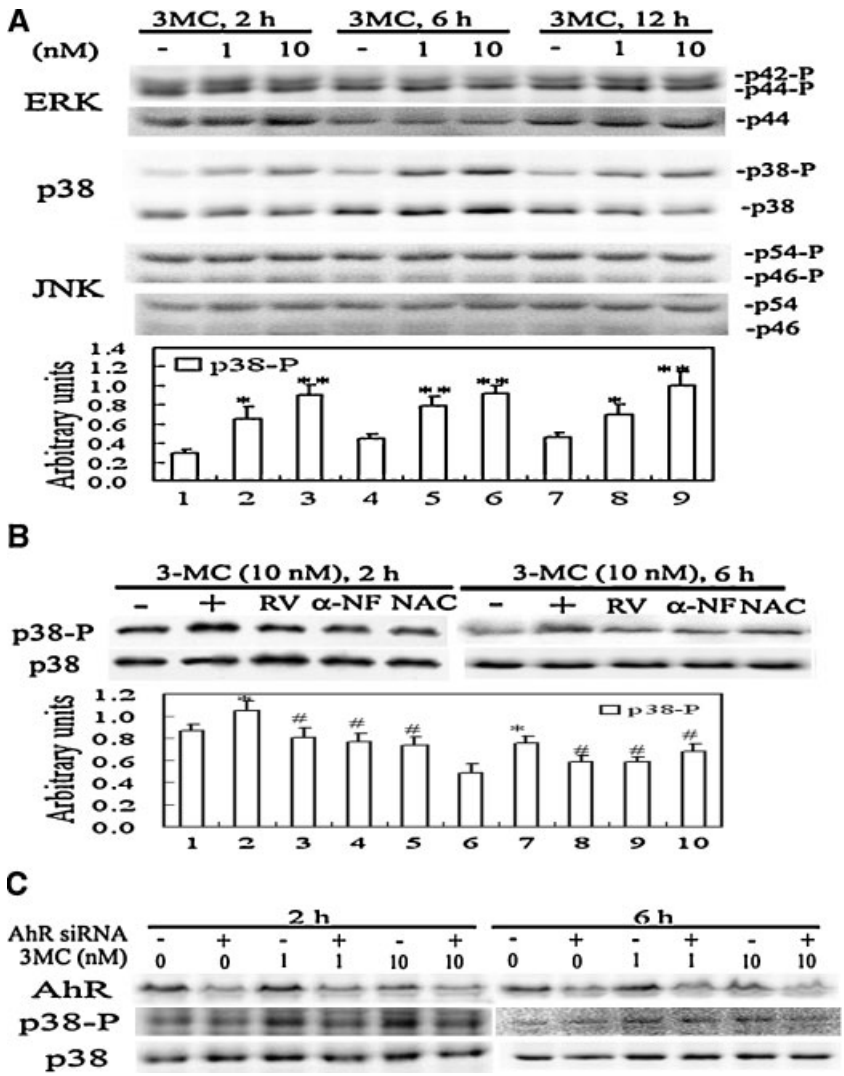

Fig. 4. Phosphorylation of p38MAPK in relation to the AhR and oxidative stress. A: Western blots of MAPKs in HUVECs exposed to 3MC. Cells were rendered quiescent for 24 h with 2% FBS, followed by treatment with DMSO and the indicated concentrations of 3MC for 2, 6, and 12 h. Individual MAPKs were identified by their size (kDa), and (P) designates phosphorylated MAPK. B: Effect of AhR antagonists and an antioxidant on the phosphorylation of p38MAPK in HUVECs exposed to 10 nM 3MC. Cells were pretreated with 2 μM resveratrol (RV), α-naphthoflavone (α-NF), or 1 mM *N*-acetylcysteine (NAC) for 1 h, prior to adding 10 nM 3MC, followed by incubation for 2 or 6 h. C, Effect of AhR knockdown on p38MAPK phosphorylation. The method was described previously in Figure 2B. Bar charts in the lower parts of parts A and B show the band intensity of normalized p38-P protein by densitometry. Data were derived from three independent experiments and are presented as the mean ± SD. $^{*}P < 0.05$ and $^{**}P < 0.01$ versus each control group. $^{\#}P < 0.05$ versus the 3MC-treated group.

until cells were pretreated with NAC, whereas the activity of the DRE-deleted p27 promoter (Dp27) was completely obliterated in response to 3MC, suggesting the importance of the DRE in the p27 promoter region obtained in this study.

Discussion

Our recent work has shown that 3MC arrests HUVECs at the G0/G1 phase of the cell cycle, and has the antiangiogenic and antiadhesive effects in HUVECs (Juan et al., 2006). In the present study, we demonstrated that p21 and p27 are mainly associated with the antiproliferative effects of 3MC in HUVECs; induction occurs through functional DRE enhancers in the promoter regions of p21 and p27, and through the concomitant activation of the p38MAPK signal transduction pathway (summarized in Fig. 8).

The most significant finding in this study is that both the AhR and activation of p38MAPK are responsible for the induction of p21 and p27. Furthermore, the time frames and effects of RV, α-NF, and NAC on p21 and p27 transactivation by 3MC suggest that the binding of the AhR to the DRE plays a direct immediate role in the induction of p21 and p27, whereas the phosphorylation of p38MAPK by AhR-dependent or -independent oxidative stress contributes to the sustained levels of p21 and p27 induction. Evidence in support of this notion was provided using AhR antagonists and antioxidants, and a deletion mutation on the putative DRE analyzed by the MOTIF Search software for transcription factor binding site analysis. RV, an

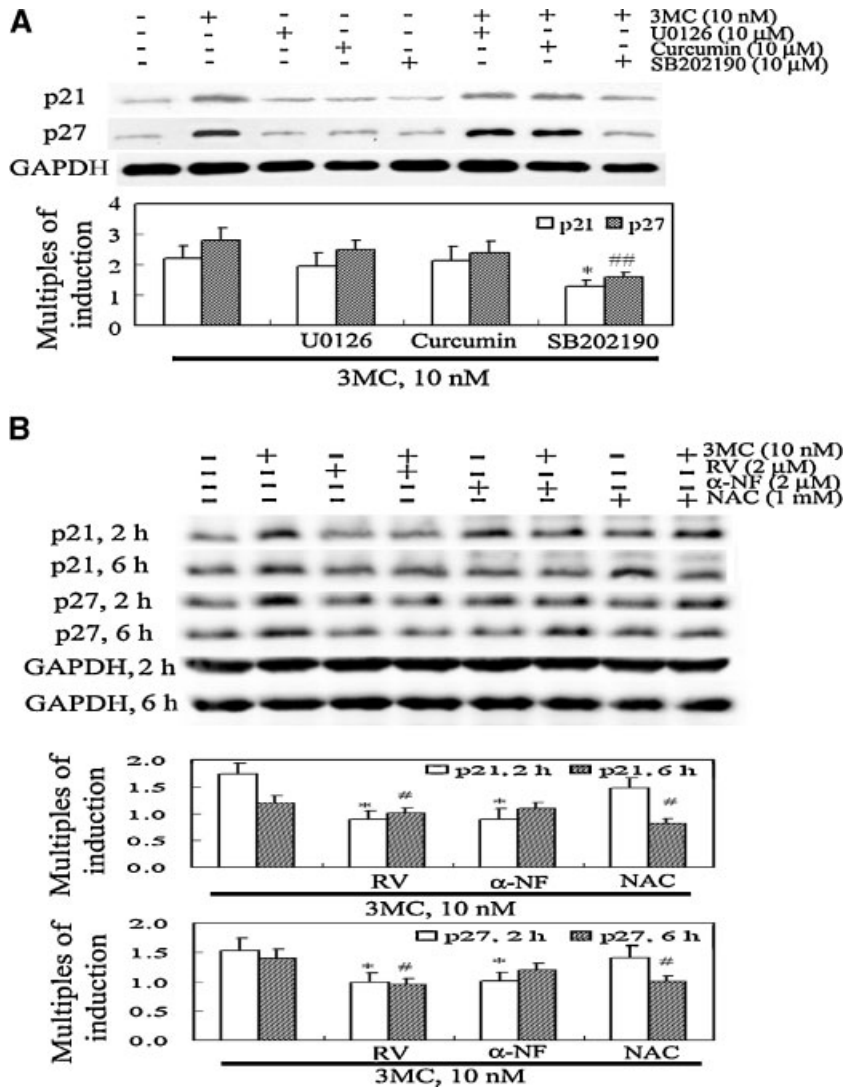

Fig. 5. Inhibition of 3MC-mediated p21 and p27 induction by blocking p38MAPK and AhR activation. A: Western blots of MAPK inhibitors on HUVECs upregulating p21 or p27 by 3MC. HUVECs were pretreated with 10 μM of each indicated MAPK inhibitor for 1 h prior to adding 10 nM 3MC, followed by incubation for another 9 h. B: Effects of AhR antagonists and NAC on early (2 h) and late (6 h) protein levels of p21 and p27 by 3MC. Cells were pretreated with 2 μM resveratrol, 2 μM α-NF, and 1 mM NAC for 1 h, followed by 10 nM 3MC treatment for 2 or 6 h. Equal loading was confirmed by incubation with an anti-GAPDH antibody. Representative results of three separate experiments are shown. Bar charts in the lower part show multiples of induction of experimental groups with respect to each individual control group after normalization with GAPDH.

AhR antagonist and antioxidant, significantly eliminated 3MC-mediated p21 promoter activity at both 2 and 6 h after 3MC treatment, whereas NAC only effectively decreased the activity at the later time point of 6 h but not at 2 h. In contrast, α-NF without reported antioxidative activity only significantly abolished the induction at the early time of 2 h, but not at 6 h. Consistent with these results, the deletion mutation of DRE in the p21 promoter did not completely alleviate 3MC-mediated activity at 6 h unless cells had been pretreated with NAC. This might suggest that there may be a DRE-independent mechanism associated with oxidative stress involved in the transcriptional regulation of p21. Based on the data presented in Figure 4C, AhR knockdown only slightly decreased phosphorylation of p38MAPK by 3MC, suggesting that an AhR-independent pathway is involved in 3MC-mediated oxidative stress. Nevertheless, the extent of the contribution of DRE or of the downstream targets of p38MAPK to the increase in 3MC-mediated p21 promoter activity remains to be further investigated.

In contrast, 3MC-mediated p27 promoter activity was significantly reversed by both RV and a deletion mutation of DRE at 2 and 6 h, but was not affected by the additional NAC treatment. This and the findings in Figure 5A,B together suggest that the obtained p27 promoter region might not respond to regulation by the relevant p38MAPK pathway, which might be explained by the smaller capacity of the p27 promoter compared to the p21 promoter for induction in response to 3MC challenge (2.0- to 2.5-fold increase for the p27 promoter vs. 3.5- to 4.0-fold increase for the p21 promoter). Additionally, our laboratory showed the evidence of the association between 3MC and oxidative stress. For instance, 3MC

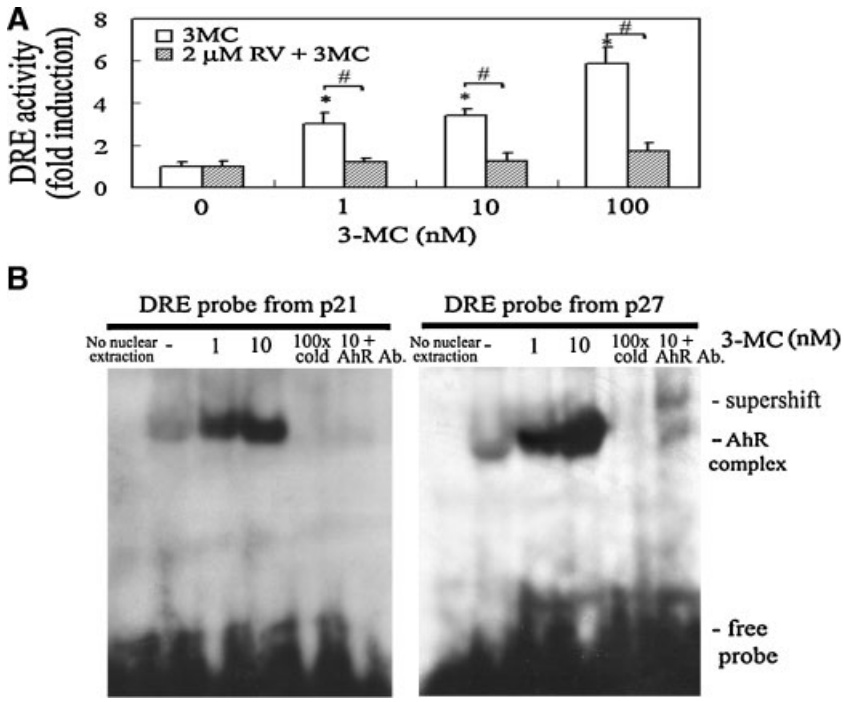

Fig. 6. Concentration-dependent effects of 3MC on DRE-driven luciferase activity with respect to resveratrol (RV) (A) and the binding activity of AhR to the putative DRE derived from the promoter regions of p21 or p27 (B). A: HUVECs were transiently transfected with the pGL2/3DRE and phRL-TK for 24 h, as described in "Materials and Methods Section." HUVECs were pretreated with 2 μM RV for 1 h prior to challenge with the indicated concentrations of 3MC. Luciferase activities of the reported plasmid were normalized to those of the internal control plasmid. Data were derived from three independent experiments and are presented as the mean ± SD. *$P < 0.05$ versus the control group. #$P < 0.05$ versus the 3MC-treated group at each corresponding concentration. B: Cells were cultured and treated with increasing concentrations of 3MC as indicated. Nuclear proteins were assayed for AhR binding activity by EMSA. 100× cold denotes a 100-fold molar excess of unlabeled oligonucleotides relative to the ^{32}P-labeled probe; this was added to the binding assay for competition with the unlabeled oligonucleotides. The mobility of specific AhR-DRE complex is indicated. Representative results of three separate experiments are shown.

concentration-dependently increases CYP1A1 induction (Juan et al., 2006). Furthermore, data presented in this study illustrated that 3MC activates p38MAPK phosphorylation, whereas SB202190 suppresses p21 and p27 upregulation by 3MC. Interestingly, it has been shown that inhibitors of p38MAPK (SB203580 and SB202190, pyridinyl imidazole compounds), block TCDD-induced CYP1A1-mRNA transcription by suppressing the recruitment of some co-activators with histone acetyltransferase activity (Shibazaki et al., 2004). Thus, we could not rule out the possibility that the suppression of 3MC-mediated p21 and p27 induction by SB212190 is independent of inhibition of MAPK activation. Likewise, how p38MAPK activation modulates the upregulation of p21 and p27 by 3MC (Fig. 4A), or conversely, how SB202190 suppresses 3MC-mediated p21 and p27 induction in HUVECs (Fig. 5A) remains to be further investigated.

The results presented in this study are partially supported by findings of Kwon et al. (2002): that ROS generated by CYP1A1 in the AhR-dependent pathway and the metabolites of PAH can activate the phosphorylation of p38MAPK, although they further demonstrated that activated p38MAPK subsequently activates phosphorylation of p53, leading to caspase-3-mediated apoptosis in HepG2 hepatoma cells. In contrast, we showed that activation of p38MAPK is associated with the sustained protein levels of p21 and p27 through a p53-independent pathway, as no subsequent p38MAPK-mediated p53 phosphorylation nor any apoptotic cell death was observed in a primary culture system using HUVECs (data not shown). In agreement with our findings of AhR and p38MAPK being involved in the antiproliferation of HUVECs, a previous study by Ito et al. (2004) claimed that both DRE-dependent and -independent mechanisms participate in constitutively active (CA)-AhR-induced growth inhibition because the A78D mutant of the CA-AhR, which is incapable of DRE-dependent transcription, only partially inhibited the growth of Jurkat T cells. Further studies are required to unravel the mechanisms of DRE-independent growth inhibition.

In the present study, we pinpoint two functional AhR responsive elements located at the promoter regions of p21 and p27, respectively, in response to 3MC challenge. Additionally, the increases in p21 and p27 levels act synergistically in the antiproliferative effects of 3MC in HUVECs, shown in Figure 3B. Furthermore, the functional AhR responsive elements in the p21/p27 promoters are responsible for the early induction of p21 and p27, whereas activation of p38MAPK through AhR-dependent or -independent oxidative stress sustained protein levels of 3MC-mediated p21 and p27 induction. Taken together, these findings concerning the antiproliferative molecular mechanisms of 3MC in HUVECs provide a theoretical basis for clinical approaches to the combined use of therapeutic agents (AhR antagonists and antioxidants) in endothelial maintenance and stroke prevention. In view of the potential protective mechanisms of RV and α-NF, it is important to fully understand their pharmacological significance in vascular pathology.

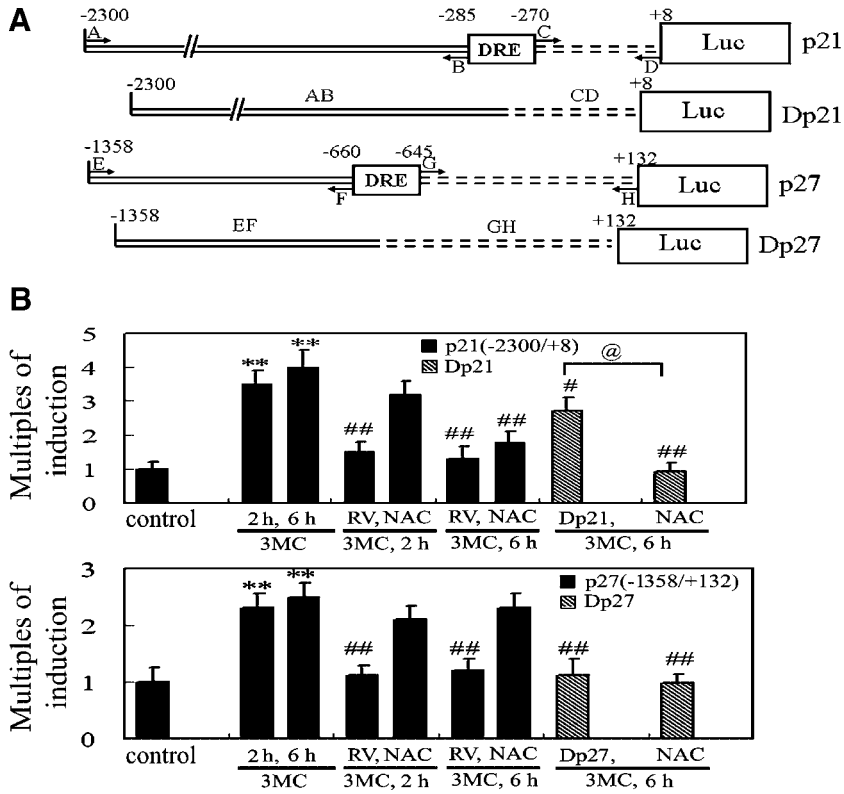

Fig. 7. 3MC-mediated p21 and p27 promoter activities in relation to DRE deletion mutation and additional resveratrol (RV) or α-naphthoflavone (α-NF) treatment. A: Deletion mutation on the putative DRE. The sequences being deleted are labeled with the DRE. The solid and broken lines indicate the template sequences on either side of the point of deletion. Four pairs of primers designated A–D for the p21 promoter, and E–H for the p27 promoter were used for PCR amplification; the resulting products of AB, CD, etc., were separately cloned into the pGL3-basic vector, as described in "Materials and Methods Section." B: HUVECs were transiently transfected with the pGL3/p21 or pGL3/p27 promoter variants and phRL-TK as an internal control plasmid for 24 h, followed by treatment with the indicated inhibitors for 1 h prior to incubation with 3MC (10 nM) for another 2 or 6 h. The activity is presented as multiples of induction for various constructs treated with 10 nM 3MC, 2 μM RV, or 1 mM NAC with respect to each individual construct treated with DMSO or PBS alone. Six samples were analyzed in each group, and values represent the mean ± SD. $^{**}P < 0.01$ vs. the DMSO group. $^{\#}P < 0.05$ and $^{\#\#}P < 0.01$ versus the 3MC-treated group at each corresponding time point. $^{@}P < 0.05$ versus the Dp21 treated with 10 nM 3MC alone.

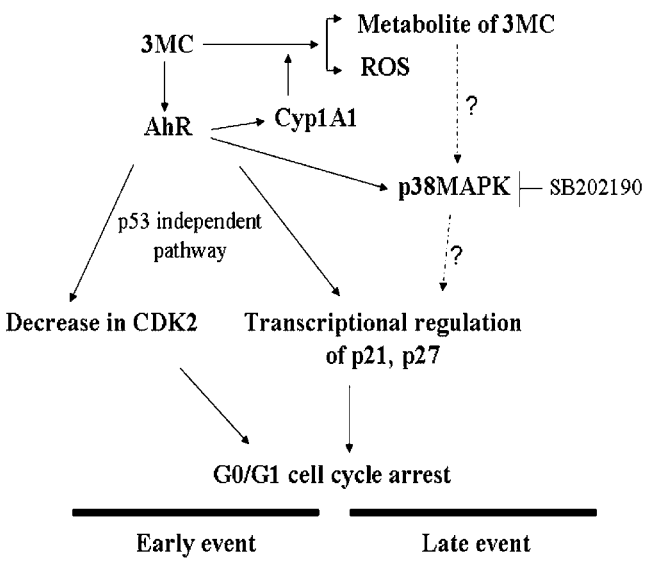

Fig. 8. A model of the molecular mechanisms of 3MC on cell cycle-related genes resulting in cell-cycle arrest. In the proposed model, activation of AhR by 3MC (early) is followed by concomitant phosphorylation of p38MAPK (late) attributed to the antiproliferation of HUVECs.

Acknowledgments

We are grateful to Dr. Vogelstein (Johns Hopkins University, Baltimore, MD) for the gift of the pWWP-luc plasmid. This study was supported by a grant (SKH-TMU-96-08) from the Shin Kong Wu Ho-Su Memorial Hospital, Taiwan; one from the Center of Excellence for Clinical Trials and Research in Neurology Specialty; and a Topnotch Stroke Research Center Grant, Ministry of Education.

Literature Cited

Afanas'ev IB, Dorozhko AI, Brodskii AV, Kostyuk VA, Potapovitch AI. 1989. Chelating and free radical scavenging mechanisms of inhibitory action of rutin and quercetin in lipid peroxidation. Biochem Pharmacol 38:1763–1769.

Bors W, Saran M. 1987. Radical scavenging by flavonoid antioxidants. Free Radic Res Commun 2:289–294.

Brouwer A, Ahlborg UG, Van den Berg M, Birnbaum LS, Boersma ER, Bosveld B, Denison MS, Gray LE, Hagmar L, Holene E, et al. 1995. Functional aspects of developmental toxicity of polyhalogenated aromatic hydrocarbons in experimental animals and human infants. Eur J Pharmacol 293:1–40.

Davis RJ. 1999. Signal transduction by the c-Jun N-terminal kinase. Biochem Soc Symp 64:1–12.

Denison MS, Whitlock JP, Jr. 1995. Xenobiotic-inducible transcription of cytochrome P450 genes. J Biol Chem 270:18175–18178.

el-Deiry WS, Tokino T, Velculescu VE, Levy DB, Parsons R, Trent JM, Lin D, Mercer WE, Kinzler KW, Vogelstein B. 1993. WAF1, a potential mediator of p53 tumor suppression. Cell 75:817–825.

Gomez N, Cohen P. 1991. Dissection of the protein kinase cascade by which nerve growth factor activates MAP kinases. Nature 353:170–173.

Han J, Lee JD, Bibbs L, Ulevitch RJ. 1994. A MAP kinase targeted by endotoxin and hyperosmolarity in mammalian cells. Science 265:808–811.

Hankinson O. 1995. The aryl hydrocarbon receptor complex. Annu Rev Pharmacol Toxicol 35:307–340.

Hoffer A, Chang CY, Puga A. 1996. Dioxin induces transcription of fos and jun genes by Ah receptor-dependent and -independent pathways. Toxicol Appl Pharmacol 141:238–247.

Ito T, Tsukumo S, Suzuki N, Motohashi H, Yamamoto M, Fujii-Kuriyama Y, Mimura J, Lin TM, Peterson RE, Tohyama C, Nohara K. 2004. A constitutively active arylhydrocarbon receptor induces growth inhibition of jurkat T cells through changes in the expression of genes related to apoptosis and cell cycle arrest. J Biol Chem 279:25204–25210.

Jaffe EA, Nachman RL, Becker CG, Minick CR. 1973. Culture of human endothelial cells derived from umbilical veins. Identification by morphologic and immunologic criteria. J Clin Invest 52:2745–2756.

Jain M, He Q, Lee WS, Kashiki S, Foster LC, Tsai JC, Lee ME, Haber E. 1996. Role of CD44 in the reaction of vascular smooth muscle cells to arterial wall injury. J Clin Invest 97:596–603.

Jin DQ, Jung JW, Lee YS, Kim JA. 2004. 2,3,7,8-Tetrachlorodibenzo-p-dioxin inhibits cell proliferation through arylhydrocarbon receptor-mediated G1 arrest in SK-N-SH human neuronal cells. Neurosci Lett 363:69–72.

Juan SH, Lee JL, Ho PY, Lee YH, Lee WS. 2006. Antiproliferative and antiangiogenic effects of 3-methylcholanthrene, an aryl-hydrocarbon receptor agonist, in human umbilical vascular endothelial cells. Eur J Pharmacol 530:1–8.

Kwon YW, Ueda S, Ueno M, Yodoi J, Masutani H. 2002. Mechanism of p53-dependent apoptosis induced by 3-methylcholanthrene: Involvement of p53 phosphorylation and p38 MAPK. J Biol Chem 277:1837–1844.

Kyriakis JM, Avruch J. 2001. Mammalian mitogen-activated protein kinase signal transduction pathways activated by stress and inflammation. Physiol Rev 81:807–869.

Lee JE, Safe S. 2001. Involvement of a post-transcriptional mechanism in the inhibition of CYP1A1 expression by resveratrol in breast cancer cells. Biochem Pharmacol 62:1113–1124.

Ma Q, Whitlock JP, Jr. 1997. A novel cytoplasmic protein that interacts with the Ah receptor, contains tetratricopeptide repeat motifs, and augments the transcriptional response to 2,3,7,8-tetrachlorodibenzo-p-dioxin. J Biol Chem 272:8878–8884.

Martinez J, Moreno JJ. 2000. Effect of resveratrol, a natural polyphenolic compound, on reactive oxygen species and prostaglandin production. Biochem Pharmacol 59:865–870.

Nebreda AR, Porras A. 2000. p38 MAP kinases: Beyond the stress response. Trends Biochem Sci 25:257–260.

Ng D, Kokot N, Hiura T, Faris M, Saxon A, Nel A. 1998. Macrophage activation by polycyclic aromatic hydrocarbons: Evidence for the involvement of stress-activated protein kinases, activator protein-1, and antioxidant response elements. J Immunol 161: 942–951.

Rorke EA, Sizemore N, Mukhtar H, Couch LH, Howard PC. 1998. Polycyclic aromatic hydrocarbons enhance terminal cell death of human ectocervical cells. Int J Oncol 13:557–563.

Safe SH. 1995. Modulation of gene expression and endocrine response pathways by 2,3,7,8-tetrachlorodibenzo-p-dioxin and related compounds. Pharmacol Ther 67:247–281.

Shibazaki M, Takeuchi T, Ahmed S, Kikuchi H. 2004. Suppression by p38 MAP kinase inhibitors (pyridinyl imidazole compounds) of Ah receptor target gene activation by 2,3,7,8-tetrachlorodibenzo-p-dioxin and the possible mechanism. J Biol Chem 279:3869–3876.

Shimada T, Hayes CL, Yamazaki H, Amin S, Hecht SS, Guengerich FP, Sutter TR. 1996. Activation of chemically diverse procarcinogens by human cytochrome P-450 1 B1. Cancer Res 56:2979–2984.

Whitlock JP, Jr, Okino ST, Dong L, Ko HP, Clarke-Katzenberg R, Ma Q, Li H. 1996. Cytochromes P450 5: Induction of cytochrome P4501A1: A model for analyzing mammalian gene transcription. FASEB J 10:809–818.

Wung BS, Cheng JJ, Hsieh HJ, Shyy YJ, Wang DL. 1997. Cyclic strain-induced monocyte chemotactic protein-1 gene expression in endothelial cells involves reactive oxygen species activation of activator protein 1. Circ Res 81:1–7.